Interaction between filler species in double-filled skutterudites

Yanyun Hu,[1] James R. Salvador,[2] Ning Chen,[3] and Young-June Kim[1,*]

[1]*Department of Physics, University of Toronto, 60 St. George Street, Toronto, Ontario M5S 1A7, Canada*
[2]*Chemical and Materials Systems Lab, General Motors R&D Center, Warren, Michigan 48090, USA*
[3]*Canadian Light Source, Saskatoon, Saskatchewan S7N 0X4, Canada*

Filled skutterudites are workhorse materials in thermoelectric research. In recent years, double- or even triple-filling has emerged as a promising strategy to improve the thermoelectric figure of merit in skutterudites. For example, one type of filler is used to reduce thermal conductivity while the other filler is used to control the electron filling. However, in these studies, each filler atom is considered independent of each other and the interaction between the two filler atoms is completely ignored. Here we present our detailed investigation of the local structure of filler atoms in $(Yb, In)_x Co_4 Sb_{12}$ and show that significant interaction does exist between filler species. While Yb or In filler atoms at low concentration occupy the usual $2a$ filler site on their own, when Yb filler concentration goes above a critical value $x \approx 0.15$, Yb pushes In atoms from the $2a$ site and into the $24g$ substitutional site replacing Sb atoms. This behavior is in stark contrast to that of Ga, which forms a dual-site defect even in the absence of Yb fillers. The temperature-dependent, extended x-ray absorption fine structure (EXAFS) data further reveal distinct lattice dynamical properties around In, Ga, and Yb filler atoms. Our findings point out that the filler interaction should be an important design consideration for new thermoelectric skutterudites.

Cobalt antimonide based skutterudite has been recognized as a candidate for large-scale applications in midtemperature thermoelectric (TE) power generation, because of its thermal stability and good TE performance [1]. Its thermoelectric properties originate from the unusual cubic crystal structure that contains two large voids which are often filled with a variety of foreign atoms: rare earths, alkaline earths, etc. An extensive investigation in the past two decades has led to a good understanding of the role played by these filler atoms; loosely bound filler atoms suppress the lattice thermal conductivity of $Co_4 Sb_{12}$ skutterudites, while allowing researchers to tune the carrier concentration without changing the band structure [2–4]. On the other hand, microscopic understanding of skutterudites in the presence of two or more types of fillers and potential interaction between these fillers is still lacking. This is unfortunate, since there has been growing interest in using more than one type of filler atom in order to fine-tune thermoelectric properties for specific applications in recent years [5–12].

Of particular interest is the group 13 fillers like Ga and In, and their interaction with additional rare-earth or alkaline-earth fillers [8,13–15]. When combined with other filler species, Ga and In seem to increase the overall solubility of fillers (dopants), allowing greater control of electronic properties such as carrier concentrations or sometimes band structure [13,15–17]. Such double-filling of skutterudites is, therefore, emerging as an effective route to modify electronic properties to achieve better thermoelectric efficiency. Due to the relatively large electronegativity of Ga and In compared to other filler species, there have been questions as to whether Ga/In goes

into the filler position ($2a$ site) or replaces Sb/Co within the skutterudite framework [18–20]. Recent experimental and theoretical studies suggest that Ga goes into both the $2a$ and $24g$ sites, forming a dual-site charge-compensated compound defect of Ga-containing samples [21–23]. However, the In case still remains controversial: some studies report In only goes into the $2a$ sites [24–26], while other studies suggest In forms a dual-site defect similar to Ga [23,27]. There have been even suggestions that In mostly forms an InSb secondary phase [14,28]. Besides, the behavior of In and Ga in the presence of another filler species is even less understood [15,17,22,23,28,29].

In this paper, we report a detailed examination of the location of filler atoms in Yb and In double-filled $Co_4 Sb_{12}$ samples by studying the element-specific local structure of Yb and In atoms. We first confirm that in single-filled samples, In occupies traditional filler sites [crystallographic $2a$ sites, see Fig. 1(a)], just like Yb single-filled samples. However, we find that the In site occupation is dramatically affected by the presence of the second filler Yb, and when the filling fraction of Yb goes above a critical value, more electronegative In atoms begin to migrate toward the $24g$ sites, replacing Sb atoms [Figs. 1(a) and 1(b)]. Our findings for the Yb-In double-filled samples contrast those in Yb-Ga double-filled samples, in which Ga exhibits partial occupancy of the $24g$ site [Figs. 1(c) and 1(d)] even in the single-filled case [30]. In addition, even when In occupies both the $2a$ and $24g$ sites, they do not form a compound defect, unlike the Ga case. Our results illustrate that the interaction between the different filler species is quite subtle, and demonstrate the importance of detailed local structure investigation of filler atoms in the double-filled skutterudite samples.

The local structure was determined using the extended x-ray absorption fine structure (EXAFS) technique, which
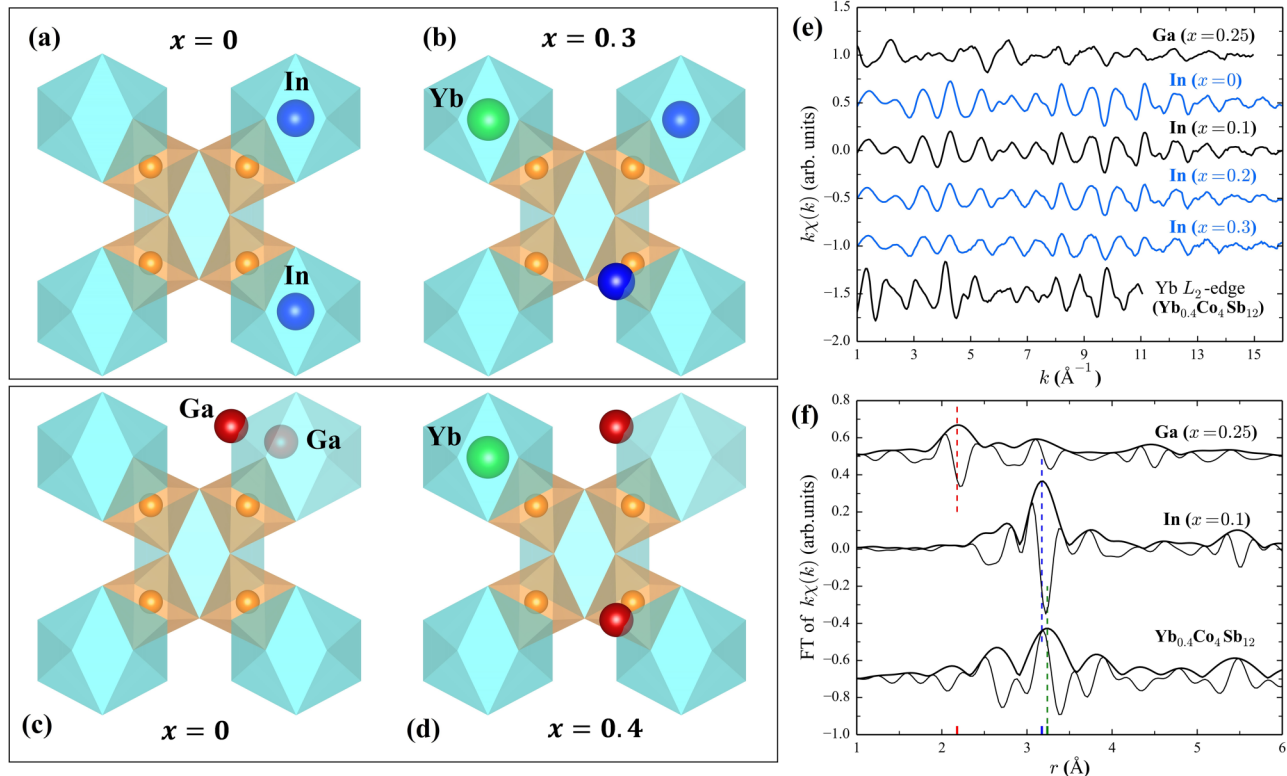
*yjkim@physics.utoronto.ca

FIG. 1. Schematic structures of (a) In single-filled $In_{0.15}Co_4Sb_{12}$ ($x = 0$) and (b) Yb-In double-filled $In_{0.15}Yb_xCo_4Sb_{12}$ when $x = 0.3$. Schematic structures for Ga single- to double-filled $Ga_{0.15}Yb_xCo_4Sb_{12}$ when (c) $x = 0$ and (d) $x = 0.4$. The unit cell is cubic (space group $Im\bar{3}$) and the void space is highlighted with an icosahedral cage structure. The Co atoms are in yellow, the Sb atoms that are making up the icosahedral cages are not shown for clarity purpose. (e) Ga K-edge k-space EXAFS data for $Ga_{0.15}Yb_{0.25}Co_4Sb_{12}$ at $T = 10$ K, In K-edge data for $In_{0.15}Yb_xCo_4Sb_{12}$ ($x = 0$ to 0.3) at $T = 20$ K, and Yb L_2-edge data for single-filled $Yb_{0.4}Co_4Sb_{12}$ at $T = 10$ K. (f) r-space EXAFS data for $Ga_{0.15}Yb_{0.25}Co_4Sb_{12}$ [labeled as Ga ($x = 0.25$)], $In_{0.15}Yb_{0.1}Co_4Sb_{12}$ [labeled as In ($x = 0.1$)] and $Yb_{0.4}Co_4Sb_{12}$. The Fourier transform (FT) ranges are 3–14 Å^{-1} for Ga, 3–15 Å^{-1} for In, and 3–10.4 Å^{-1} for Yb. The fast oscillating function is the real part (Re) of the FT, while the envelope function is the magnitude of the FT, i.e., $\sqrt{Re^2 + Im^2}$ with Im the imaginary part (not shown) of the FT.

uses photoexcited electrons as probing particles. When the x-ray energy is sufficient to excite one of the core electrons to the continuum state of the atom of interest, the thus-generated photoelectron propagates toward neighboring atoms and backscatter from them. This backscattered photoelectron will interfere (constructively or destructively) with another photoelectron from the originating atom, modulating the absorption spectra. Examples of such EXAFS oscillations plotted as a function of photoelectron momentum (k) are shown in Fig. 1(e). Interpretation of the EXAFS signal usually requires Fourier transformation (FT) of the data from k-space into real space (r-space). The so-obtained r-space data consist of several pair-distribution peaks corresponding to interatomic distances; for quantitative information, curve-fitting to theoretical standards provided by the FEFF code was carried out in the ARTEMIS software [31–33].

Polycrystalline $In_{0.15}Yb_xCo_4Sb_{12}$ ($x = 0, 0.05, 0.1, 0.2, 0.3$) were synthesized by induction melting the elements in stoichiometric ratio in a sealed vial at 1200 °C for 5 min. The resulting charges were melt spun by heating to 1200 °C and subsequently ejected onto a copper wheel spinning at a tangential wheel speed of 20 m/s. The recovered ribbons were cold pressed and then heat treated under an inert atmosphere at 650 °C for 4 hr. The absence of impurities in the samples was confirmed by x-ray powder diffraction at room temperature.

Rietveld analysis revealed the cubic skutterudite structure, and the lattice parameters are shown in the Supplemental Material [34].

All EXAFS experiments were carried out in fluorescence mode on the hard x-ray microanalysis (HXMA) beamline 06ID-1 at the Canadian Light Source (CLS). The sample preparation procedures for EXAFS measurements had been described in Ref. [30]. For the In K-edge (27940 eV) measurements, a double-crystal Si(220) monochromator was used and the higher harmonic rejection was achieved by a 20% detuning of the second crystal. Indium K-edge data were collected for all In-containing samples at $T = 20$ K, by using an Oxford liquid helium cryostat. Temperature-dependent EXAFS spectra were collected for the $In_{0.15}Yb_xCo_4Sb_{12}$ ($x = 0.2$) sample from 20 to 280 K. The temperature was stabilized within ± 0.5 K. At least three spectra were recorded at each temperature for each sample. The x-ray absorption measurements at Ga K-edge (10367 eV) for the nominal $Ga_{0.15}Yb_{0.25}Co_4Sb_{12}$ has been described in detail in the previous room-temperature studies [30]. Temperature dependence of the Ga K-edge EXAFS spectra was collected from 10 to 300 K. For comparison, Yb L_2-edge EXAFS data for one single-filled sample ($Yb_{0.4}Co_4Sb_{12}$) were also collected from 10 to 300 K.

In Fig. 1(f), we display the EXAFS profiles in r-space around Ga, In, and Yb atoms for the double-filled

$Ga_{0.15}Yb_xCo_4Sb_{12}$ ($x = 0.25$) and $In_{0.15}Yb_xCo_4Sb_{12}$ ($x = 0.1$), and single-filled $Yb_{0.4}Co_4Sb_{12}$ compounds, respectively. The main peak position clearly shows a large variation in r-space: ~ 2.2 Å for Ga and $r \sim 3.2$ Å for In and Yb. This indicates that the local environment of the In or Yb atom differs substantially from that of Ga. The observed difference of less than 0.1 Å between In and Yb is due to the different lattice parameters, which were obtained independently from x-ray powder diffraction measurements (see Supplemental Material [34]). Since the In K-edge EXAFS data for the ($x = 0$) and ($x = 0.1$) samples of $In_{0.15}Yb_xCo_4Sb_{12}$ are almost identical as displayed in Fig. 1(e) and the r-space curve-fitting results are the same, we will use the ($x = 0.1$) data as representative of the ($x = 0$), ($x = 0.1$), and ($x = 0.05$) (not shown) samples in the following analyses.

The EXAFS data for the Yb or In single-filled sample can be fitted very well with the model in which Yb/In occupies the center of the voids ($2a$ site), as shown in Fig. 2(a) (see Supplemental Material [34] for fitting details). This reveals that as a single filler species, both Yb and In occupy the on-center $2a$ site exclusively in the $Yb_{0.4}Co_4Sb_{12}$ and $In_{0.15}Co_4Sb_{12}$ samples, which is consistent with the findings in many other rare-earth-filled skutterudites [35,36]. However, among the Yb-In double-filled skutterudites, particularly when the Yb concentration increases to $x = 0.2$, the In K-edge EXAFS amplitude decreases for the $InYb(x = 0.2)$ and even smaller for $InYb(x = 0.3)$ as shown in Fig. 1(e), suggesting that either the local environment of In becomes disordered or different types of In local environments coexist. In Fig. 2(b), we demonstrated that our attempt to fit the In($x = 0.2$) data with the $2a$-site-only model (purple lines) is unsatisfactory. In particular, significant deviation from the fitting in the $r \sim 2.2$ Å region was found, as shown in the dashed box [a negative bowl-shaped signal in the real part, which is absent in Fig. 2(a) as for In($x = 0.1$)]; this indicates additional contributions from different scattering paths are required for In($x = 0.2$). A dual-site (red lines) model, in which a fraction of In atoms are located at the $24g$ site while the rest remains at the $2a$ site, was used to fit the data for the In($x = 0.2$) and In($x = 0.3$) samples [Fig. 2(b)]. In this model, the EXAFS features around $r \sim 2.2$ Å are attributed to the In_{24g}-Co single path (blue lines); the overall fit (red lines) presents a significant improvement in the fit quality as determined by the Hamilton F-test confidential level of 0.99. The Hamilton F-test uses the ratio of χ_v^2 parameters and the number of degrees of freedom for two fits, to determine if one is significantly better [37].

Another piece of evidence indicating dual-site occupancy of In is the difference in the temperature dependence of features associated with the $2a$ and $24g$ sites. In Fig. 3(a), two data sets for In($x = 0.3$) obtained at 20 and 300 K are compared. The first peak (~ 2.2 Å) is associated with In in the $24g$-site (In_{24g}-Co path), while the strong peak (~ 3.2 Å) is due to In in the $2a$-site (In_{24g}-Co path). As the sample is warmed from 20 to 300 K, the amplitude of the 3.2 Å peak decreases by more than 75% while that of the 2.2 Å peak drops by only 40%. The uneven ratio for these two peaks suggests that In occupies two different sites, and that the lattice vibrational properties of these sites are dramatically different as we show below.

Figure 3(b) summarizes the fit results of the $2a$ site fraction for the In in the Yb-In double-filled skutterudites as a function
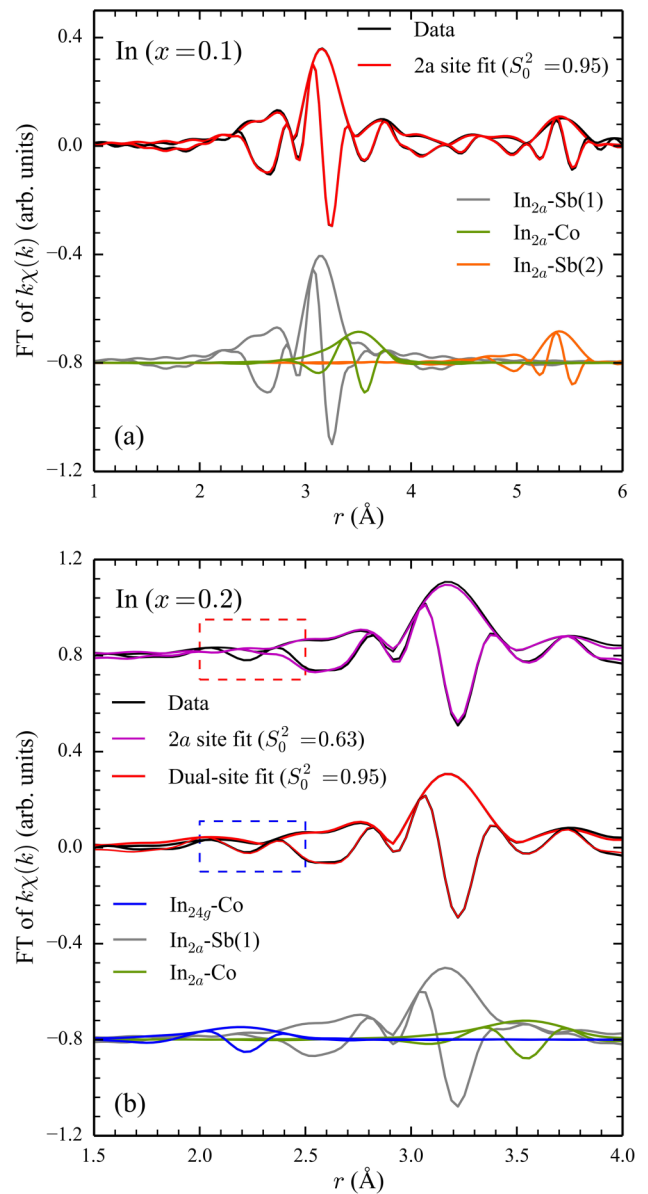

FIG. 2. (a) Fit result for the In ($x = 0.1$) compound and various single-scattering path contributions; $2a$ site model is used to fit the data. Fit range is 1–6 Å. (b) Comparison of fits for the In ($x = 0.2$) sample in the r-range of 1.5–4 Å. Fit quality is significantly improved when using the dual-site (In_{24g} and In_{2a}) model instead of the $2a$ site only model. The In_{24g}-Co single-path contribution explains the real part feature at $r \sim 2.2$ Å (dashed box region).

of Yb content x. Interestingly, we found that In dopants occupy the on-center $2a$ site exclusively in the Co_4Sb_{12} skutterudite structure for $x = 0$ to $x = 0.1$, while the In_{2a} fraction starts to decrease for $x > 0.1$. In Fig. 3(b), we also reproduced the fraction of Ga in the $2a$ site in Yb-Ga double-filled skutterudites reported in Ref. [30]. In contrast to the In case, the fraction of Ga_{2a} shows a gradually decreasing trend from 2/3 at $x = 0$ to zero at $x = 0.4$. In all Ga-containing samples, some fraction of Ga always occupies the $24g$ site. Our result unambiguously shows that the additional Yb fillers have an important direct impact on the position of Ga and In dopants.
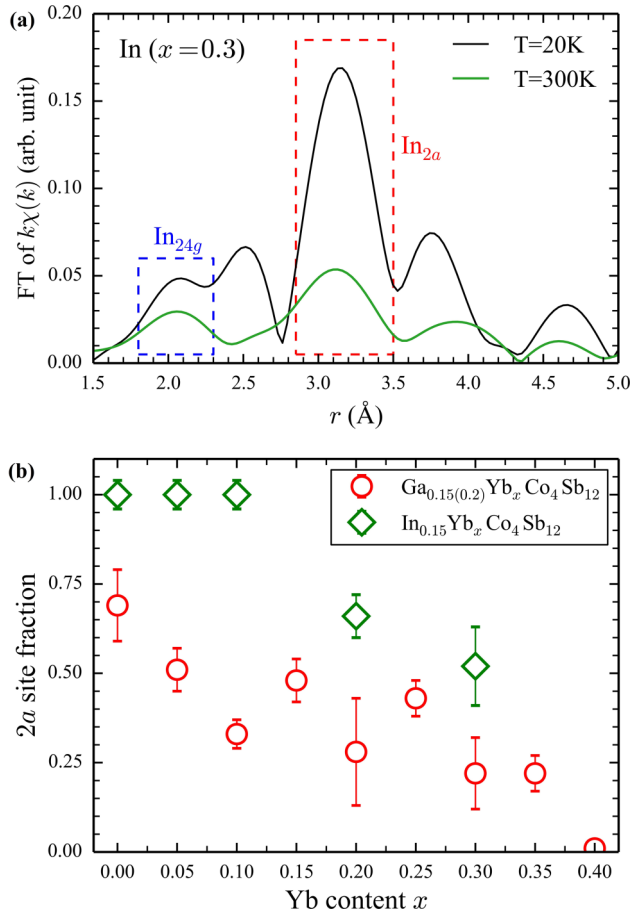
FIG. 3. (a) r-space EXAFS magnitude variation for $In_{0.15}Yb_xCo_4Sb_{12}$ ($x = 0.3$): In_{24g} vs In_{2a} peaks show uneven ratios when the sample is warmed from 20 to 300 K. The FT was taken in the range of 3–10 Å^{-1} for both datasets. (b) Summary of $2a$ site fraction as a function of the Yb content x for $M_{0.15}Yb_xCo_4Sb_{12}$ ($M=$ In or Ga). Note that In_{2a} atoms are on-center while Ga_{2a} atoms are strongly displaced from the center position.

FIG. 4. (a) Comparison of the temperature dependence of the mean-square displacements [$\sigma^2(T)$] for the nearest In_{2a}-Sb, In_{24g}-Co of the In($x = 0.2$) sample, and Ga_{2a}-Ga_{24g} and Ga_{24g}-Co of the Ga($x = 0.25$) sample. Also included for comparison are the Yb_{2a}-Sb results obtained from Yb L_2-edge data for $Yb_{0.4}Co_4Sb_{12}$. Solid lines are fits to an Einstein or a correlated Debye model. (b) Guest species such as Yb/In (m, in blue) loosely bound inside the cage framework (M, in cyan) when the spring constants $k_2 \ll k_1$, and impurity atom such as Ga doping defect (m, in red) replacing at the cage framework site with a modified spring constant $k_1' \approx k_1$.

In addition to the fractional occupancy, the dynamical properties of Ga and In fillers are quite different as illustrated in the temperature dependence. It is known in EXAFS that the instability of the local structure around the absorber atoms can be interpreted by the mean-square displacement (σ^2) of the atom-pair distance, and the temperature dependence of σ^2 contains information of the lattice dynamical properties for the near neighboring atom pairs. Figure 4(a) exhibits the variation of σ^2 with T for various atom pairs in the GaYb($x = 0.25$) and InYb($x = 0.2$) samples. The Yb-only sample data are also plotted for comparison. The values of $\sigma^2(T)$ show very strong temperature dependence for In in the $2a$ site, which is quite similar to that of the Yb_{2a}. On the other hand, the temperature dependence of the $\sigma^2(T)$ of Ga and In in the $24g$ site is not very strong. It is also interesting to note that the Ga_{2a}-Ga_{24g} bond shows only weak temperature dependence.

Filler atoms (such as Ce) in filled skutterudites are often modeled with an independent rattler inside a cage [35,38]. Such a rattler can be approximated as a harmonic oscillator, i.e., Einstein model; and $\sigma^2(T)$ due to thermal vibration, $\sigma_{vib,E}^2$, in
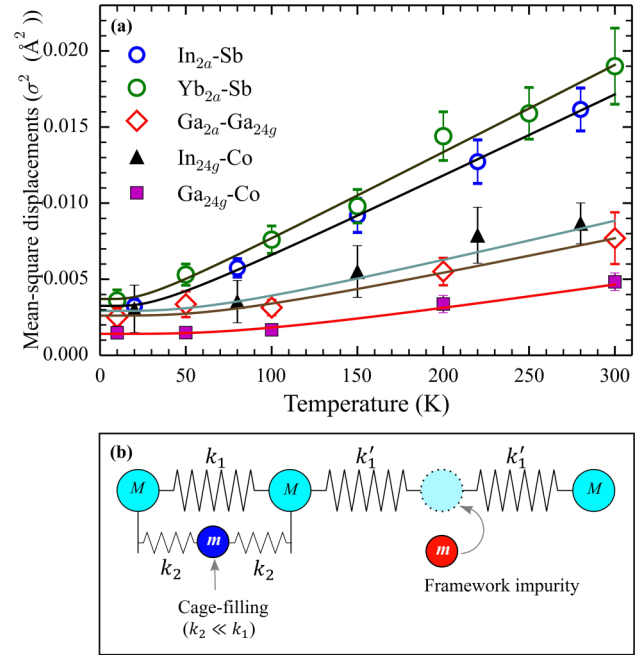
this model is given as [39,40]

$$\sigma_{\text{vib},E}^2(T) = \frac{\hbar^2}{2\mu k_B \Theta_E} \coth \frac{\Theta_E}{2T}, \tag{1}$$

where μ denotes the reduced mass of the Einstein oscillator atom, Θ_E is the Einstein temperature of this vibration mode, k_B is the Boltzmann constant, and $\hbar$ is the reduced Planck constant. The total mean-squared displacement is this vibration component and the static component combined: $\sigma^2(T) = \sigma_{\text{vib},E}^2(T) + \sigma_{\text{static}}^2$. The so-obtained static offset is indistinguishable from zero within experimental uncertainties for the In_{2a}-Sb pair. The low values in σ_{static}^2 indicates a high degree of uniformity in the position of In_{2a} throughout the sample, and also that the equilibrium position of In_{2a} is at the cage center at low T, in agreement with the low T results for the other rare-earth fillers occupying the on-center position in the skutterudite voids [36,41,42]. The somewhat larger value of σ_{static}^2 for Yb_{2a} is probably due to the statistics of the relatively higher filling concentration of Yb. The Einstein temperatures are 89 ± 5 and 70 ± 5 K for the In_{2a}-Sb and Yb_{2a}-Sb pairs, respectively, corresponding to the low-lying local vibrational modes observed in the inelastic neutron scattering [43,44]. The difference between Θ_E(In) and Θ_E(Yb) is almost entirely due to the mass difference: $\Theta_E(\text{In})/\Theta_E(\text{Yb}) \approx \sqrt{m(\text{Yb})/m(\text{In})}$, since a lighter mass atom vibrates with a higher frequency inside the cage.

In contrast, the variation of σ^2 with T for Ga_{2a}-Ga_{24g}, Ga_{24g}-Co, and In_{24g}-Co are relatively weak. To quantify their

TABLE I. Fit results for σ^2 vs T for the near neighboring atom pairs extracted from the In K-edge data for the In$_{0.15}$Yb$_{0.2}$Co$_4$Sb$_{12}$, Ga K-edge for the Ga$_{0.15}$Yb$_{0.25}$Co$_4$Sb$_{12}$, and Yb L_2-edge for the Yb$_{0.4}$Co$_4$Sb$_{12}$. For the Einstein model (e.g., for In$_{2a}$-Sb and Yb$_{2a}$-Sb), the reduced mass μ in each fit was set to be the filler ion atomic mass while in the correlated Debye model, $\mu = \mu_1\mu_2/(\mu_1 + \mu_2)$ where μ_1 and μ_2 are the atomic masses in that atom pair. Estimated systematic errors for Θ_E are ± 5 K and for Θ_D are ± 30 K; errors for σ^2_{static} are about 0.0004 Å^2.

Atom pair	μ	Θ_E (K)	Θ_D (K)	σ^2_{static} (Å^2)
In$_{2a}$-Sb	114.8	89		0.0008
In$_{24g}$-Co	39.0		250	0.0005
Ga$_{24g}$-Co	31.9		350	0.0000
Ga$_{2a}$-Ga$_{24g}$	34.9		280	0.0002
Yb$_{2a}$-Sb	173.0	70		0.0017

lattice dynamics, a correlated Debye model was used to fit the σ^2 vs T for each atom pair to extract the corresponding Debye temperature Θ_D. The correlated Debye model is given by [39,40]

$$\sigma^2_D(T) = \frac{3\hbar}{2\omega^3\mu} \int_0^{\omega_D} d\omega\, \omega \coth(\hbar\omega/2k_BT)$$
$$\times \left(1 - \frac{\sin(\omega r_{ij}q_D/\omega_D)}{\omega r_{ij}q_D/\omega_D}\right), \qquad (2)$$

where ω_D is the Debye frequency, $q_D (= (6\pi^2 N/V)^{1/3})$ is the Debye wave vector, and μ is the reduced mass of an atom pair with distance r_{ij}. The fit results are shown in Fig. 4(a) as solid lines; the values for Debye temperature, $\Theta_D (= \hbar\omega_D/k_B)$, are summarized in Table. I. Again σ^2_{static} was small and close to zero. The Debye temperature of $\Theta_D = 350 \pm 30$ K and $\Theta_D = 250 \pm 30$ K for Ga$_{24g}$-Co and In$_{24g}$-Co indicate that these bonds are fairly stiff, which is expected from the fact that the nearest Sb-Co in a Co$_4$Sb$_{12}$ lattice forms a strong covalent bond and the lattice itself exhibits good thermal stability at high T [36]. However, the Debye temperature for the Ga$_{2a}$-Ga$_{24g}$ bond is surprisingly high, 280 ± 30 K, as compared to the $\Theta_E = 89 \pm 5$ K for the In$_{2a}$-Sb, suggesting that the low-lying rattling mode observed for In$_{2a}$ does not exist for Ga$_{2a}$. Instead Ga$_{2a}$ seems to form a strong covalent bond with the neighboring Ga$_{24g}$ atom, as proposed for a charge-compensated compound defect model [21].

The observed difference between the local structures of Ga and In in these double-filled skutterudites has crucial implications for lattice thermal conductivity, κ_l, in these compounds. We introduce a heuristic one-dimensional spring model shown in Fig. 4(b) in order to discuss the role of In$_{2a}$ and In$_{24g}$ type fillers in suppressing κ_l. In the first case, the periodic Co$_4$Sb$_{12}$ framework units (M, in cyan) are strongly bonded with each other with a spring constant k_1, and the filler atoms such as In$_{2a}$ and Yb$_{2a}$ (m, in blue) are loosely bound with a weak spring interaction ($k_2 \ll k_1$). In this case, the framework acoustic phonon mode will weakly interact with the local vibrating (i.e., rattling) mode of the filler atom, exhibiting avoided crossing behavior, and its group velocity will be greatly suppressed near the rattling frequency ($\sim \sqrt{(k_2/m)}$), leading to suppression of κ_l [45,46]. On the other hand, in the second case, impurity

atoms such as the In$_{24g}$ and Ga$_{24g}$ (m, in red) are incorporated into the Sb framework and form mass defects, ignoring a small modification in the spring constant. Such a mass defect will generate a localized mode [47], which can scatter off acoustic phonons. Since the mass difference between Ga and Sb is much more substantial than that between In and Sb, we expect more prominent suppression of κ_l due to Ga defects in this case.

Our experimental findings then suggest completely distinct mechanisms for the suppression of lattice thermal conductivity in Ga-Yb and In-Yb double-filled skutterudites, and provide plausible explanations for the doping dependence of κ_l reported in Refs. [16,48]. That is, κ_l for the Yb-Ga double-filled skutterudites decreases more rapidly as a function of additional Yb content x at low x and remains smaller at high x, when compared to that of Yb-In double-filled compounds (see Supplemental Material [34] for the κ_l comparison). In the Yb-Ga double-filled compounds, we found no evidence of Ga cage-filling rattling mode, evidenced by the lack of strong temperature dependence of Ga EXAFS. This suggests that the κ_l suppression is entirely due to the second mechanism discussed above and that the dramatic increase of Ga$_{24g}$ with Yb from $x = 0$ to $x = 0.1$ [see Fig. 3(b)] is the main reason for the strong suppression of κ_l. On the other hand, the reduction of κ_l in the Yb-In double-filled skutterudites is due to the rattling vibration of the cage fillers as has been proposed for other filled skutterudites [5]. However, this mechanism is only valid for $x < 0.1$, since additional In does not go to a $2a$ site and replaces Sb instead. The second mechanism, which should kick in at higher doping levels, apparently is not as effective in reducing κ_l, probably due to the similar atomic masses of In and Sb (6% difference).

To summarize, we have compared the local structure and local dynamics around In, Ga, and Yb dopants in a series of $M_{0.15}$Yb$_x$Co$_4$Sb$_{12}$ (M= In or Ga) skutterudites by measuring the EXAFS data at the In K-, Ga K- and Yb L_2-edges, respectively. We found that in both Yb-Ga and Yb-In double-filled skutterudites the local structure of Ga and In are subject to the filling concentration of the secondary filler, Yb. However, contrary to the Ga dopants which form dual-site defects at the single-filling level ($x = 0$), our results show that both Yb and In occupy the on-center $2a$ site exclusively in their single-filled samples. The fraction of In$_{2a}$ starts to decrease at $x = 0.2$, resulting in about half of the In on the $24g$ substitutional sites in the In ($x = 0.3$). The temperature-dependent EXAFS results provide further evidence that the In$_{2a}$, very similar to the normal rattler Yb, is loosely bound inside the cage and vibrates as an Einstein oscillator at a low frequency $\Theta_E = 89 \pm 5$ K. This is distinct from the Ga$_{2a}$ which forms a stiff bond with the cage atoms at a Debye temperature $\Theta_D = 280 \pm 30$ K. This EXAFS study has presented an excellent example of interaction between filler species even in the limit of dilute concentrations in complex compounds. Full investigation of the lattice and electronic transports for the double- or multiple-filled skutterudites should take into account the interaction between different filler species and the similarities and differences in their filling and doping behaviors.

[1] G. Rogl and P. Rogl, Curr. Opinion Green Sustain. Chem. **4**, 50 (2017).

[2] G. A. Slack, in *CRC Handbook of Thermoelectrics*, edited by D. M. Rowe (CRC, Boca Raton, FL, 1995), pp. 407–440.

[3] B. C. Sales, D. Mandrus, B. C. Chakoumakos, V. Keppens, and J. R. Thompson, Phys. Rev. B **56**, 15081 (1997).

[4] Y. Tang, Z. M. Gibbs, L. A. Agapito, G. Li, H.-S. Kim, M. B. Nardelli, S. Curtarolo, and G. J. Snyder, Nat. Mater. **14**, 1223 (2015).

[5] J. Yang, W. Zhang, S. Q. Bai, Z. Mei, and L. D. Chen, Appl. Phys. Lett. **90**, 192111 (2007).

[6] L. Xi, J. Yang, W. Zhang, L. Chen, and J. Yang, J. Am. Chem. Soc. **131**, 5560 (2009).

[7] X. Shi, J. Yang, J. R. Salvador, M. Chi, J. Y. Cho, H. Wang, S. Bai, J. Yang, W. Zhang, and L. Chen, J. Am. Chem. Soc. **133**, 7837 (2011).

[8] S. R. S. Kumar, D. Cha, and H. N. Alshareef, J. Appl. Phys. **110**, 083710 (2011).

[9] J. R. Salvador, J. Yang, H. Wang, and X. Shi, J. Appl. Phys. **107**, 043705 (2010).

[10] L. Guo, X. Xu, J. R. Salvador, and G. P. Meisner, Appl. Phys. Lett. **102**, 111905 (2013).

[11] G. Rogl, A. Grytsiv, K. Yubuta, S. Puchegger, E. Bauer, C. Raju, R. Mallik, and P. Rogl, Acta Mater. **95**, 201 (2015).

[12] M. Rull-Bravo, A. Moure, J. F. Fernandez, and M. Martin-Gonzalez, RSC Adv. **5**, 41653 (2015).

[13] J. Y. Peng, P. N. Alboni, J. He, B. Zhang, Z. Su, T. Holgate, N. Gothard, and T. M. Tritt, J. Appl. Phys. **104**, 053710 (2008).

[14] H. Li, X. Tang, Q. Zhang, and C. Uher, Appl. Phys. Lett. **94**, 102114 (2009).

[15] J. Peng, W. Xu, Y. Yan, J. Yang, L. Fu, H. Kang, and J. He, J. Appl. Phys. **112**, 024909 (2012).

[16] X. Shi, J. Yang, L. Wu, J. R. Salvador, C. Zhang, W. L. Villaire, D. Haddad, J. Yang, Y. Zhu, and Q. Li, Sci. Rep. **5**, 14641 (2015).

[17] W. Zhao, P. Wei, Q. Zhang, C. Dong, L. Liu, and X. Tang, J. Am. Chem. Soc. **131**, 3713 (2009).

[18] X. Shi, W. Zhang, L. D. Chen, and J. Yang, Phys. Rev. Lett. **95**, 185503 (2005).

[19] A. Harnwunggmoung, K. Kurosaki, T. Plirdpring, T. Sugahara, Y. Ohishi, H. Muta, and S. Yamanaka, J. Appl. Phys. **110**, 013521 (2011).

[20] R. C. Mallik, E. Mueller, and I.-H. Kim, J. Appl. Phys. **111**, 023708 (2012).

[21] Y. Qiu, L. Xi, X. Shi, P. Qiu, W. Zhang, L. Chen, J. R. Salvador, J. Y. Cho, J. Yang, Y.-C. Chien, S.-W. Chen, Y. Tang, and G. J. Snyder, Adv. Funct. Mater. **23**, 3194 (2013).

[22] Y. Qiu, J. Xing, X. Gao, L. Xi, X. Shi, H. Gu, and L. Chen, J. Mater. Chem. A **2**, 10952 (2014).

[23] L. Xi, Y. Qiu, S. Zheng, X. Shi, J. Yang, L. Chen, D. J. Singh, J. Yang, and W. Zhang, Acta Mater. **85**, 112 (2015).

[24] T. He, J. Chen, H. D. Rosenfeld, and M. A. Subramanian, Chem. Mater. **18**, 759 (2006).

[25] W. Zhao, P. Wei, Q. Zhang, H. Peng, W. Zhu, D. Tang, J. Yu, H. Zhou, Z. Liu, X. Mu, D. He, J. Li, C. Wang, X. Tang, and J. Yang, Nat. Commun. **6**, 7197 (2015).

[26] E. Visnow, C. P. Heinrich, A. Schmitz, J. de Boor, P. Leidich, B. Klobes, R. P. Hermann, W. E. Müller, and W. Tremel, Inorg. Chem. **54**, 7818 (2015).

[27] Y. Tang, Y. Qiu, L. Xi, X. Shi, W. Zhang, L. Chen, S.-M. Tseng, S.-W. Chen, and G. J. Snyder, Energy Environ. Sci. **7**, 812 (2014).

[28] J. Graff, S. Zhu, T. Holgate, J. Peng, J. He, and T. M. Tritt, J. Electron. Mater. **40**, 696 (2011).

[29] W. Zhao, Z. Liu, Z. Sun, Q. Zhang, P. Wei, X. Mu, H. Zhou, C. Li, S. Ma, D. He, P. Ji, W. Zhu, X. Nie, X. Su, X. Tang, B. Shen, X. Dong, J. Yang, Y. Liu, and J. Shi, Nature **549**, 247 (2017).

[30] Y. Hu, N. Chen, J. P. Clancy, J. R. Salvador, C.-Y. Kim, X. Shi, Q. Li, and Y.-J. Kim, Phys. Rev. B **96**, 224107 (2017).

[31] J. J. Rehr, E. A. Stern, R. L. Martin, and E. R. Davidson, Phys. Rev. B **17**, 560 (1978).

[32] J. J. Rehr, J. J. Kas, F. D. Vila, M. P. Prange, and K. Jorissen, Phys. Chem. Chem. Phys. **12**, 5503 (2010).

[33] B. Ravel and M. Newville, J. Synchrotron Radiat. **12**, 537 (2005).

[34] See Supplemental Material at http://link.aps.org/supplemental/10.1103/PhysRevMaterials.2.082401 for x-ray diffraction re-sults, comparison of lattice thermal conductivities, and addi-tional EXAFS data and analyses.

[35] D. Cao, F. Bridges, P. Chesler, S. Bushart, E. D. Bauer, and M. B. Maple, Phys. Rev. B **70**, 094109 (2004).

[36] F. Bridges, Mod. Phys. Lett. B **30**, 1630001 (2016).

[37] L. Downward, C. H. Booth, W. W. Lukens, and F. Bridges, AIP Conf. Proc. **882**, 129 (2007).

[38] K. Nitta, Y. Omori, T. Miyanaga, K. Takegahara, H. Sugawara, D. Kikuchi, and H. Sato, J. Phys. Soc. Jpn. **82**, 044801 (2013).

[39] G. Dalba and P. Fornasini, J. Synchrotron Radiat. **4**, 243 (1997).

[40] M. Vaccari and P. Fornasini, J. Synchrotron Radiat. **13**, 321 (2006).

[41] D. Wee, B. Kozinsky, N. Marzari, and M. Fornari, Phys. Rev. B **81**, 045204 (2010).

[42] N. Bernstein, J. L. Feldman, and D. J. Singh, Phys. Rev. B **81**, 134301 (2010).

[43] I. K. Dimitrov, M. E. Manley, S. M. Shapiro, J. Yang, W. Zhang, L. D. Chen, Q. Jie, G. Ehlers, A. Podlesnyak, J. Camacho, and Q. Li, Phys. Rev. B **82**, 174301 (2010).

[44] M. M. Koza, M. Boehm, E. Sischka, W. Schnelle, H. Mutka, and A. Leithe-Jasper, Phys. Rev. B **91**, 014305 (2015).

[45] M. Christensen, A. B. Abrahamsen, N. B. Christensen, F. Juranyi, J. Andersen, C. R. H. Bahl, and B. B. Iversen, Nat. Mater. **7**, 811 (2008).

[46] E. S. Toberer, A. Zevalkink, and G. J. Snyder, J. Mater. Chem. **21**, 15843 (2011).

[47] J. M. Ziman, in *Principles of the Theory of Solids*, 2nd ed. (Cambridge University, New York, 1972), pp. 211–254.

[48] J. Peng, J. He, Z. Su, P. N. Alboni, S. Zhu, and T. M. Tritt, J. Appl. Phys. **105**, 084907 (2009).